Published in final edited form as:
Cell Metab. 2012 February 8; 15(2): 240–246. doi:10.1016/j.cmet.2011.12.017.

The Scap/SREBP Pathway Is Essential for Developing Diabetic Fatty Liver and Carbohydrate-Induced Hypertriglyceridemia in Animals

Young-Ah Moon[1,4], **Guosheng Liang**[1,4], **Xuefen Xie**[1], **Maria Frank-Kamenetsky**[3], **Kevin Fitzgerald**[3], **Victor Koteliansky**[3], **Michael S. Brown**[1], **Joseph L. Goldstein**[1], and **Jay D. Horton**[1,2,*]

[1]Department of Molecular Genetics, University of Texas Southwestern Medical Center, Dallas, TX 75390-9046, USA

[2]Department of Internal Medicine, University of Texas Southwestern Medical Center, Dallas, TX 75390-9046, USA

[3]Alnylam Pharmaceuticals, 300 Third Street, Cambridge, MA 02142, USA

SUMMARY

Insulin resistance leads to hypertriglyceridemia and hepatic steatosis and is associated with increased SREBP-1c, a transcription factor that activates fatty acid synthesis. Here, we show that steatosis in insulin-resistant *ob*/*ob* mice was abolished by deletion of Scap, an escort protein necessary for generating nuclear isoforms of all three SREBPs. Scap deletion reduced lipid synthesis and prevented fatty livers despite persistent obesity, hyperinsulinemia, and hyperglycemia. Scap deficiency also prevented steatosis in mice fed high-fat diets. Steatosis was also prevented when siRNAs were used to silence Scap in livers of sucrose-fed hamsters, a model of diet-induced steatosis and hypertriglyceridemia. This silencing reduced all three nuclear SREBPs, decreasing lipid biosynthesis and abolishing sucrose-induced hypertriglyceridemia. These results demonstrate that SREBP activation is essential for development of diabetic hepatic steatosis and carbohydrate-induced hypertriglyceridemia, but not insulin resistance. Inhibition of SREBP activation has therapeutic potential for treatment of hypertriglyceridemia and fatty liver disease.

INTRODUCTION

SREBPs are transcription factors that activate the synthesis of fatty acids (FAs), triglycerides (TGs), and cholesterol in all organs (Horton et al., 2002). In liver, hyperactivation of SREBPs causes TG accumulation (Shimomura et al., 1999a), producing the pathological condition known as hepatic steatosis, which can lead to cirrhosis and liver failure (Cohen et al., 2011). In liver, the primary activator of SREBPs is insulin, which increases the synthesis and proteolytic processing of one of the three SREBP isoforms, namely SREBP-1c (Brown and Goldstein, 2008; Shimomura et al., 1999b). The most frequent cause of hepatic steatosis is obesity, which leads to insulin resistance and a

*Correspondence: jay.horton@utsouthwestern.edu.
[4]These authors contributed equally to this work

SUPPLEMENTAL INFORMATION

Supplemental Information includes two figures, two tables, Supplemental Experimental Procedures, and Supplemental References and can be found with this article online at doi:10.1016/j.cmet.2011.12.017.

compensatory increase in plasma insulin. In rodent models of obesity, a paradox arises. Although the liver resists one action of insulin—namely, suppression of gluconeogenesis, it remains sensitive to the other action—namely, stimulation of SREBP-1c (Brown and Goldstein, 2008). Thus, when insulin levels rise, the hormone hyperactivates SREBP-1c and hepatic steatosis ensues.

SREBPs are synthesized as membrane-bound precursors in the endoplasmic reticulum (ER) that must be processed in order to activate transcription (Brown and Goldstein, 2009). Immediately after synthesis, SREBPs form complexes with Scap, an ER-to-Golgi transport protein. In the Golgi, SREBPs are processed sequentially by two proteases that release the transcriptionally active fragment of SREBPs. The released SREBP fragments enter the nucleus where they activate transcription of all genes necessary to convert acetyl-CoA to FAs and cholesterol (Horton et al., 2002). Scap is essential for SREBP processing. In cultured cells lacking Scap (Rawson et al., 1999) and in livers of Scap knockout mice (Matsuda et al., 2001), SREBP precursors are rapidly degraded, and they never reach the Golgi for processing and thus never enter the nucleus.

The SREBP family includes three isoforms with separate, but overlapping functions. SREBP-1a activates cholesterol and FA synthesis. It is abundant in growing cells, but is expressed at relatively low levels in liver (Shimomura et al., 1997). SREBP-1c, abundant in liver, primarily activates FA synthesis, while the other abundant hepatic isoform, SREBP-2, activates cholesterol production (Horton et al., 2002). SREBP-2 also activates the gene encoding the LDL receptor (LDLR), which increases cholesterol uptake into liver, and PCSK9, a secreted protein that degrades hepatic LDLRs, thereby reducing cholesterol uptake (Horton et al., 2009).

Although previous studies, largely correlative in nature, have postulated a central role for SREBPs in obesity-induced TG accumulation in liver and blood, the hypothesis has not been tested rigorously for two reasons: (1) at high levels of expression, SREBP-2 can activate FA synthesis (Horton et al., 1998); and (2) selective knockout of the SREBP-1c isoform or both SREBP-1a and -1c isoforms results in a marked compensatory increase in SREBP-2 expression in livers of mice, thus blocking the overall effect on FA synthesis (Liang et al., 2002; Shimano et al., 1997).

The logical way to test the SREBP hypothesis is to eliminate all SREBPs in liver and then determine whether this ameliorates TG accumulation in liver and plasma in models of insulin resistance. Inasmuch as the functions of the three SREBP isoforms partially overlap, removal of all SREBP actions in liver would require the elimination of all three SREBP isoforms. In the current studies, we eliminated all nuclear SREBPs at once by deleting the Scap protein, which is required for all SREBP processing. We used two approaches in two animal models: (1) liver-specific deletion of *Scap* by homologous recombination in *ob*/*ob* mice, an animal model of severe obesity, insulin resistance, and hepatic steatosis; and (2) knockdown of Scap mRNA through RNAi in livers of sucrose-fed hamsters, a model of carbohydrate-induced hypertriglyceridemia (Avramoglu et al., 2003; Taghibiglou et al., 2000). The combined results provide strong evidence for an essential role of SREBPs in activating pathological lipogenesis in response to hyperinsulinemia or carbohydrate overload.

RESULTS

Deletion of SREBP-1c Only Partially Reduces Liver Fat in *ob*/*ob* Mice

In humans and mice with insulin resistance and hepatic steatosis, SREBP-1c levels and FA synthesis rates are elevated in liver (Donnelly et al., 2005; Higuchi et al., 2008; Shimomura

et al., 1999a). To determine if blocking SREBP-1c activity is sufficient to prevent the development of hepatic steatosis in insulin-resistant states, we deleted SREBP-1c from *ob*/*ob* mice, which become massively obese and insulin resistant owing to a mutation in *leptin* (Zhang et al., 1994). Unexpectedly, inactivation of the *Srebp-1c* isoform in *ob*/*ob* mice reduced hepatic FA synthesis and TG content by only ~50% (Figure S1). This partial reduction in liver TG had no impact on plasma insulin, glucose, or body weights of *ob*/*ob* mice (data not shown).

Liver-Specific Deletion of *Scap* Prevents Hepatic Steatosis in *ob*/*ob* Mice

To determine if blocking all SREBP activity in liver is required to prevent the induction of lipogenesis and hepatic steatosis in an insulin-resistant state, we used a previously described line of mice with floxed *Scap* alleles (Matsuda et al., 2001). We bred these mice with *albumin-Cre* transgenic mice to achieve liver-specific inactivation of *Scap* (*L-Scap*$^{-}$). *L-Scap*$^{-}$ mice were crossed with *ob*/*ob* mice to generate *ob*/*ob;L-Scap*$^{-}$ mice.

Scap was undetectable in immunoblots of liver extracts from *L-Scap*$^{-}$ and *ob*/*ob;L-Scap*$^{-}$ mice (Figure 1A). Immunoblotting with an antibody that detects both SREBP-1a and -1c revealed an elevation in the nuclear SREBP-1 in *ob*/*ob* mice. Previous studies showed that this is attributable to an increase in the synthesis and processing of SREBP-1c, which is stimulated by hyperinsulinemia in these mice (Shimomura et al., 1999a; Shimomura et al., 1999b). Nuclear forms of all SREBPs were not detectable in any of the Scap-deficient mice. The membrane-bound SREBP precursors were also markedly reduced in *L-Scap*$^{-}$ mice, in part because of a 90% reduction in SREBP-1c mRNA and a 50% reduction in SREBP-2 mRNA (Table S1). It is also likely that the precursors were rapidly degraded as previously observed in Scap-deficient CHO cells (Rawson et al., 1999).

As previously reported for *ob*/*ob* mice, mRNAs for FA synthetic enzymes ACC-1 and FAS were markedly elevated in *ob*/*ob* mouse livers (Shimomura et al., 1999a; Shimomura et al., 1999b), and this increase was abolished in *ob*/*ob;L-Scap*$^{-}$ mice (Figure 1B). The mRNAs for other SREBP target genes were also reduced. These included elongation of very long chain fatty acids 6 (Elovl6), stearoyl CoA desaturase-1 (SCD-1), HMG-CoA synthase, and HMG-CoA reductase (Figure 1B).

To confirm the functional significance of the mRNA reductions, we measured hepatic FA synthesis in vivo using ^{3}H-water (Figure 2A). FA synthesis was markedly elevated in livers of *ob*/*ob* mice, and this was reduced by nearly 90% when Scap was absent. We noted that Scap deficiency also lowered FA synthesis even in WT mice. Liver TG content was elevated by 10-fold in *ob*/*ob* mice, reflecting severe hepatic steatosis (Figure 2B). Remarkably, these levels were reduced to normal in *ob*/*ob;L-Scap*$^{-}$ mice. Scap deficiency also reduced hepatic TGs in WT mice. Liver weights were increased in *ob*/*ob* mice and were reduced toward normal in *ob*/*ob;L-Scap*$^{-}$ mice (Figures 2C and 2D). The enlarged livers of *ob*/*ob* mice were pale in color, owing to TG accumulation (Figure 2G). The color was normalized in *ob*/*ob;L-Scap*$^{-}$ mice (Figure 2H).

Figures 2B–2F and Table S1 present relevant metabolic parameters in the mice under study. Although Scap deficiency abolished overproduction of TGs in *ob*/*ob* livers, it had no effect on food intake or body weight. At 12 weeks of age, body weights were similarly elevated in *ob*/*ob* and *ob*/*ob;L-Scap*$^{-}$ mice (53.2 and 47.4 g, respectively, compared with 26.5 g in WT mice) (Figure 2D). Total fat mass was also similar in *ob*/*ob* and *ob*/*ob;L-Scap*$^{-}$ mice (49.9% and 49.4% of body weight, respectively, compared with 9.3% in WT mice) (Table S1). Plasma insulin levels remained markedly elevated (47-fold and 34-fold in *ob*/*ob* and *ob*/*ob;L-Scap*$^{-}$, respectively) (Figure 2E). Despite the massive increase in plasma insulin,

plasma glucose was slightly elevated in both *ob*/*ob* lines as compared with WT (Figure 2F), indicating massive resistance to the glucose-lowering effects of insulin.

To confirm that insulin resistance was not altered by deleting Scap, glucose and insulin tolerance tests were performed. We found nearly identical impairment to both challenges in *ob*/*ob* and *ob*/*ob;L-Scap*$^{-}$ mice (Figures S2A and S2B). Hyperinsulinemia present in *ob*/*ob* and *ob*/*ob;L-Scap*$^{-}$ mice also failed to suppress the expression of the gluconeogenic genes PEPCK and glucose 6-phosphatase (Table S1), again indicating a persistence of insulin resistance.

We next examined whether deletion of *Scap* also prevents hepatic steatosis, which develops in obesity induced by a high-fat diet (HFD). For these studies, we used a previously described inducible liver deletion of *Scap* that was mediated by Cre driven by the MX1 promoter (*L-Scap*$^{-}$;MX1-Cre) (Matsuda et al., 2001). Chow-fed WT and *L-Scap*$^{-}$;MX1-Cre mice (male, 12 weeks old) were treated with four intraperitoneal injections of 300 μg polyI:polyC (1 mg/ml in water) administered every 2 days to activate the MX-1 promoter and induce Cre expression in liver (Matsuda et al., 2001). After the final injection, mice were either continued on chow or fed a HFD containing 58% kcal lard and 25.6% kcal carbohydrates for 4 months prior to study. In WT mice, the HFD increased liver TG content 6-fold (from 24 to 142 mg/g) and cholesterol content 2.4-fold (from 2.2 to 5.2 mg/g) (Figures S2C and S2D). In contrast, *L-Scap*$^{-}$ mice fed the HFD had liver TG and cholesterol concentrations that were not different from WT mice fed chow (Figures S2C and S2D). In addition, WT and *L-Scap*$^{-}$ mice fed the HFD had similar elevations of plasma insulin and glucose (Figures S2E and S2F).

RNAi Silencing of Scap Ameliorates Dyslipidemia in Sucrose-Fed Hamsters

To determine whether liver Scap deficiency would reduce plasma TGs in an animal model of carbohydrate-induced hypertriglyceridemia, we studied sucrose-fed hamsters. As compared with mice, hamster lipoprotein metabolism more closely resembles that in humans because hamsters, like humans, secrete only apoB-100 containing VLDL from liver and because their plasma contains cholesteryl ester transfer protein (CETP) (Taghibiglou et al., 2000). Previous studies showed that a high carbohydrate diet raises the concentration of TGs in liver and plasma of these animals (Avramoglu et al., 2003; Taghibiglou et al., 2000). To eliminate hepatic Scap mRNA in hamsters, we delivered siRNA to liver by intravenous injection of siRNA complexed with lipid nanoparticles (LNP) (Akinc et al., 2009). In preliminary experiments, we designed a series of Scap siRNAs and screened them for their ability to decrease Scap mRNA in primary hamster hepatocytes. The most potent siRNA reduced Scap mRNA by more than 80%, and this was used for in vivo studies (designated siScap). As a control, we introduced four mutations into siScap to generate a mismatch version that did not reduce Scap mRNA (designated siScap-mm).

Hamsters were fed the high-sucrose diet for 7 weeks. On weeks 4 and 6 of the diet, hamsters were injected intravenously with saline or 2.5 mg/kg body weight of LNP-formulated siScap or siScap-mm. siScap reduced liver Scap mRNA by 80% (Table S2), and Scap protein was reduced below the limit of detection by our antibody (Figure 3A). The precursor and nuclear forms of SREBP-1 and -2 were also markedly reduced (Figure 3A). Although LDLR mRNA was reduced by siScap (Figure 3B), the level of LDLR protein did not decline (Figure 3A). LDLR preservation is likely attributable to the marked reduction in the mRNA encoding PCSK9 in these animals (Figure 3B). PCSK9 is a protein that destroys hepatic LDLRs (Horton et al., 2009). *PCSK9* and *LDLR* are both activated by SREBP-2 (Horton et al., 2003).

In the sucrose-fed hamsters, mRNAs for FAS and SCD-1, two targets of SREBP-1c, were elevated when compared to controls (indicated by the dashed line in Figure 3B). These mRNAs were reduced to normal by siScap. siScap also reduced the mRNA for ACC-1, but the reduction did not reach the level of significance at $p < 0.01$ (Table S2). The mRNAs for two cholesterol-synthesizing enzymes, HMG-CoA synthase and HMG-CoA reductase, were also reduced by siScap (Figure 3B). Control siScap-mm had none of these effects.

Plasma TGs were elevated nearly 3-fold to 570 mg/dl in sucrose-fed hamsters (Figure 4A). siScap reduced these levels nearly to normal. Liver TGs were elevated more modestly, and were reduced by siScap. siScap-mm had none of these effects. Fractionation of plasma lipoproteins by fast performance liquid chromatography (FPLC) revealed a marked reduction in VLDL-TGs and VLDL-cholesterol in siScap-treated hamsters (Figure 4C). There was no significant change in LDL- or HDL-cholesterol levels. In siScap-treated hamsters, VLDL secretion was reduced by 40% as measured by the rate of increase in plasma TGs following administration of the lipoprotein lipase inhibitor Tyloxapol (Figure 4D) (Schotz et al., 1957). As shown in Table S2, siScap treatment of sucrose-fed hamsters did not significantly affect body weight, plasma insulin levels, or blood glucose levels. siSCAP, but not siSCAP-mm, produced a statistically significant reduction in plasma free FA levels.

DISCUSSION

In the current studies, we show that elimination of nuclear SREBPs in liver ameliorates pathologic TG accumulation in three models: (1) *ob*/*ob* mice, a model of insulin resistance, metabolic syndrome, and diabetes; (2) HFD-induced insulin resistance; and (3) sucrose-fed hamsters, a model of carbohydrate-induced hypertriglyceridemia. Nuclear SREBPs were eliminated in liver by a reduction in the mRNA encoding Scap, a protein that is essential for the proteolytic activation of all SREBPs (Rawson et al., 1999). As a result, there was a corresponding decline in the mRNAs encoding essential enzymes of FA synthesis, all of whose transcription is driven by SREBPs.

In *ob*/*ob* mice, elimination of the hepatic *Scap* gene by homologous recombination produced a dramatic decline in FA synthesis and a reversal of hepatic steatosis. Improvement occurred even though the *ob*/*ob;L-Scap*$^{-}$ mice consumed excess food just like the *ob*/*ob* mice, exhibited the same gross obesity, and developed a similar massive degree of hyperinsulinemia and glucose intolerance. These data demonstrate that hepatic FA overproduction is not required for the development of systemic insulin resistance in mice.

Given the reduction in hepatic FA synthesis in *ob*/*ob;L-Scap*$^{-}$ mice, some tissue must increase its FA synthesis in order for these animals to accumulate the same excessive amount of body fat stores as *ob*/*ob* mice. Previously, we showed that the decreased hepatic FA synthesis in livers of *L-Scap*$^{-}$ mice is balanced by a compensatory increase in nonhepatic tissues, primarily adipose tissue (Kuriyama et al., 2005). The same compensatory increase also occurs in the white adipose tissue of *ob*/*ob;L-Scap*$^{-}$ mice. As shown in Table S1, the levels of lipogenic gene mRNAs in the epididymal fat pads of *ob*/*ob;L-Scap*$^{-}$ mice were increased by 1.6- to 2.5-fold compared to *ob*/*ob* mice. In the sucrose-fed hamsters, the major manifestation was a major increase in plasma VLDL-TGs with a lesser, but significant, accumulation of fat in the liver. We lowered liver Scap mRNA in these hamsters by injection of an siRNA that targets Scap. As in the *ob*/*ob* mice, a reduction in hepatic Scap led to an absence of detectable nuclear SREBPs in liver and a reduction in the mRNAs encoding FA-synthesizing enzymes. The rate of VLDL secretion from liver declined, and plasma TGs returned nearly to normal. Thus, elimination of nuclear SREBPs prevents the hypertriglyceridemia induced by carbohydrate excess in hamsters.

The hamster studies help to answer a question raised by earlier studies of hepatic SREBPs. Inasmuch as SREBP-2 activates the gene for the LDLR (Horton et al., 2002), it was theoretically possible that a decrease in nuclear SREBP would lead to an undesirable increase in plasma LDL. Indeed, we did observe a fall in LDLR mRNA in the siScap-treated hamsters (Figure 3B), but the LDLR protein did not decline (Figure 3A). We speculate that LDLR protein levels were maintained because SREBP-2 also activates the gene encoding PCSK9, a protein that destroys hepatic LDLRs (Horton et al., 2009). In mice, hepatic PCSK9 mRNA and plasma PCSK9 levels were reduced by more than 80% in *L-Scap*$^{-}$ and *ob/ob;L-Scap*$^{-}$ mice (Table S1). In the siScap-treated hamster livers, the decline in PCSK9 mRNA was at least as profound as the decline in LDLR mRNA. The net result was that LDL-cholesterol did not change in the siScap-treated hamsters (Figure 4C). If a similar result occurs in humans, it would seem that blockade of hepatic nuclear SREBPs may not lead to an undesirable decrease in LDLR protein or a rise in plasma LDL cholesterol levels.

The relevance of the current studies to humans lies in the observation that humans with hepatic steatosis manifest elevated hepatic levels of SREBP-1c (Higuchi et al., 2008) and increased rates of hepatic lipogenesis (Donnelly et al., 2005). Thus, in humans Scap is a potential target for therapies aiming to prevent hepatic steatosis and hypertriglyceridemia. Scap is a good target because so far its only known role is to escort SREBPs to the Golgi. Nuclear SREBPs might also be eliminated by inhibitors of the two proteases that process SREBPs, but this approach is likely to lead to unwanted side effects, since these proteases are required for processing of other proteins such as ATF6 and the CREB-like proteins (Ye, 2011). Further human studies will reveal whether Scap elimination has the same desirable effects in humans as it does in the two animal models studied here.

EXPERIMENTAL PROCEDURES

Animals

Mice carrying the floxed *Scap* allele (*Scap*$^{f/f}$) (Matsuda et al., 2001) were back-crossed five times into the C57BL/6J background using Marker-Assisted “Speed” Congenics and crossed with *Albumin-Cre* transgenic mice (Jackson Laboratory, No. 003574) to generate *Scap*$^{f/f}$;*Alb-Cre* mice (designated *L-Scap*$^{-}$). *L-Scap*$^{-}$ mice were bred with *lep*$^{+/ob}$ heterozygous mice (Jackson Laboratory, No. 000632) to produce *L-Scap*$^{-}$;*lep*$^{+/ob}$ mice, which were crossed to each other to obtain *ob/ob;L-Scap*$^{-}$ mice. All mice were housed in colony cages with a 12 hr light/12 hr dark cycle and fed ad libitum Harlan Teklad Rodent Diet 7002 prior to study. Golden Syrian hamsters (Harlan Laboratories) were housed in colony cages and maintained on a 12 hr light/ 12 hr dark cycle and fed Harlan Teklad Rodent Diet 7001 prior to initiation of studies. All animal experiments were performed with approval of the Institutional Animal Care and Research Advisory Committee at UT Southwestern.

Metabolic Parameters

Plasma and liver analytes were measured using previously published assays. See Supplemental Experimental Procedures for details.

In Vivo siRNA Experiments

Sequence of siScap: 5′-GCUUAAUGGUUCCCUUGAUTT-3′ (sense) and 5′-AUCAAGGGAACCAUUAAGCTT-3′ (antisense). Sequence of siScap-mm: 5′-GCUUAAUcGUaCCgUaGAUTT-3′ (sense) and 5′-AUCuAcGGuACgAUU AAGCTT-3′ (antisense), where the four mutations are denoted by lower cases. For in vivo experiments, siRNA oligos were formulated in lipid nanoparticles (LNP) (Frank-Kamenetsky et al., 2008). Golden Syrian hamsters (male, ~90 g) were fed an ad libitum chow diet (Harlan

Teklad, No. 7001) or a high-sucrose diet (MP Biomedicals diet, No. 90238) for a total of 7 weeks prior to study. On weeks 4 and 6, hamsters were injected via jugular vein with saline or with 2.5 mg/kg body weight of LNP-formulated siScap or siScap-mm. One week after the final injection, hamsters were fasted for 4 hr and euthanized with saturating isoflurane to obtain plasma and tissues for analyses.

Quantitative Real-Time PCR

Total RNA was extracted from each liver using RNA STAT-60 (Tel-Test, Inc.) and subjected to quantitative real-time PCR as described (Liang et al., 2002). Primers for mouse genes were described previously (Liang et al., 2002; Yang et al., 2001); primers for hamster genes are available upon request.

Immunoblot Analyses of Liver Nuclear Extracts and Membrane Fractions

Membrane and nuclear extract fractions were prepared from five to seven mouse or hamster livers and equal aliquots from each were pooled (total, 20 μg for membranes and 30 μg for nuclear extracts) and subjected to 8% SDS-PAGE and immunoblot analyses (Engelking et al., 2004; Matsuda et al., 2001; Shimano et al., 1997).

Supplementary Material

Refer to Web version on PubMed Central for supplementary material.

Acknowledgments

This work was supported by grants from the Moss Heart Foundation and the National Institutes of Health HL-20948 and DK081182. The authors thank Norma Anderson, Tuyet Dang, Katherine Lim, Monica Mendoza, Judy Sanchez, and Isis Soto for technical assistance and Akin Akinc, Muthiah Manoharan, Martin Maier, and Satya Kuchimanchi at Alnylam for formulations and chemistry.

References

Akinc A, Goldberg M, Qin J, Dorkin JR, Gamba-Vitalo C, Maier M, Jayaprakash KN, Jayaraman M, Rajeev KG, Manoharan M, et al. Development of lipidoid-siRNA formulations for systemic delivery to the liver. Mol Ther. 2009; 17:872–879. [PubMed: 19259063]

Avramoglu RK, Qiu W, Adeli K. Mechanisms of metabolic dyslipidemia in insulin resistant states: deregulation of hepatic and intestinal lipoprotein secretion. Front Biosci. 2003; 8:d464–d476. [PubMed: 12456312]

Brown MS, Goldstein JL. Selective versus total insulin resistance: a pathogenic paradox. Cell Metab. 2008; 7:95–96. [PubMed: 18249166]

Brown MS, Goldstein JL. Cholesterol feedback: from Schoenheimer's bottle to Scap's MELADL. J Lipid Res Suppl. 2009; 50:S15–S27.

Cohen JC, Horton JD, Hobbs HH. Human fatty liver disease: old questions and new insights. Science. 2011; 332:1519–1523. [PubMed: 21700865]

Donnelly KL, Smith CI, Schwarzenberg SJ, Jessurun J, Boldt MD, Parks EJ. Sources of fatty acids stored in liver and secreted via lipoproteins in patients with nonalcoholic fatty liver disease. J Clin Invest. 2005; 115:1343–1351. [PubMed: 15864352]

Engelking LJ, Kuriyama H, Hammer RE, Horton JD, Brown MS, Goldstein JL, Liang G. Overexpression of Insig-1 in the livers of transgenic mice inhibits SREBP processing and reduces insulin-stimulated lipogenesis. J Clin Invest. 2004; 113:1168–1175. [PubMed: 15085196]

Frank-Kamenetsky M, Grefhorst A, Anderson NN, Racie TS, Bramlage B, Akinc A, Butler D, Charisse K, Dorkin R, Fan Y, et al. Therapeutic RNAi targeting PCSK9 acutely lowers plasma cholesterol in rodents and LDL cholesterol in nonhuman primates. Proc Natl Acad Sci USA. 2008; 105:11915–11920. [PubMed: 18695239]

Higuchi N, Kato M, Shundo Y, Tajiri H, Tanaka M, Yamashita N, Kohjima M, Kotoh K, Nakamuta M, Takayanagi R, Enjoji M. Liver X receptor in cooperation with SREBP-1c is a major lipid synthesis regulator in nonalcoholic fatty liver disease. Hepatol Res. 2008; 38:1122–1129. [PubMed: 18684130]

Horton JD, Shimomura I, Brown MS, Hammer RE, Goldstein JL, Shimano H. Activation of cholesterol synthesis in preference to fatty acid synthesis in liver and adipose tissue of transgenic mice overproducing sterol regulatory element-binding protein-2. J Clin Invest. 1998; 101:2331–2339. [PubMed: 9616204]

Horton JD, Goldstein JL, Brown MS. SREBPs: activators of the complete program of cholesterol and fatty acid synthesis in the liver. J Clin Invest. 2002; 109:1125–1131. [PubMed: 11994399]

Horton JD, Shah NA, Warrington JA, Anderson NN, Park SW, Brown MS, Goldstein JL. Combined analysis of oligonucleotide microarray data from transgenic and knockout mice identifies direct SREBP target genes. Proc Natl Acad Sci USA. 2003; 100:12027–12032. [PubMed: 14512514]

Horton JD, Cohen JC, Hobbs HH. PCSK9: a convertase that coordinates LDL catabolism. J Lipid Res Suppl. 2009; 50:S172–S177.

Kuriyama H, Liang G, Engelking LJ, Horton JD, Goldstein JL, Brown MS. Compensatory increase in fatty acid synthesis in adipose tissue of mice with conditional deficiency of SCAP in liver. Cell Metab. 2005; 1:41–51. [PubMed: 16054043]

Liang G, Yang J, Horton JD, Hammer RE, Goldstein JL, Brown MS. Diminished hepatic response to fasting/refeeding and liver X receptor agonists in mice with selective deficiency of sterol regulatory element-binding protein-1c. J Biol Chem. 2002; 277:9520–9528. [PubMed: 11782483]

Matsuda M, Korn BS, Hammer RE, Moon YA, Komuro R, Horton JD, Goldstein JL, Brown MS, Shimomura I. SREBP cleavage-activating protein (SCAP) is required for increased lipid synthesis in liver induced by cholesterol deprivation and insulin elevation. Genes Dev. 2001; 15:1206–1216. [PubMed: 11358865]

Rawson RB, DeBose-Boyd R, Goldstein JL, Brown MS. Failure to cleave sterol regulatory element-binding proteins (SREBPs) causes cholesterol auxotrophy in Chinese hamster ovary cells with genetic absence of SREBP cleavage-activating protein. J Biol Chem. 1999; 274:28549–28556. [PubMed: 10497220]

Schotz MC, Scanu A, Page IH. Effect of triton on lipoprotein lipase of rat plasma. Am J Physiol. 1957; 188:399–402. [PubMed: 13411223]

Shimano H, Horton JD, Hammer RE, Shimomura I, Brown MS, Goldstein JL. Overproduction of cholesterol and fatty acids causes massive liver enlargement in transgenic mice expressing truncated SREBP-1a. J Clin Invest. 1996; 98:1575–1584. [PubMed: 8833906]

Shimano H, Shimomura I, Hammer RE, Herz J, Goldstein JL, Brown MS, Horton JD. Elevated levels of SREBP-2 and cholesterol synthesis in livers of mice homozygous for a targeted disruption of the SREBP-1 gene. J Clin Invest. 1997; 100:2115–2124. [PubMed: 9329978]

Shimomura I, Shimano H, Horton JD, Goldstein JL, Brown MS. Differential expression of exons 1a and 1c in mRNAs for sterol regulatory element binding protein-1 in human and mouse organs and cultured cells. J Clin Invest. 1997; 99:838–845. [PubMed: 9062340]

Shimomura I, Bashmakov Y, Horton JD. Increased levels of nuclear SREBP-1c associated with fatty livers in two mouse models of diabetes mellitus. J Biol Chem. 1999a; 274:30028–30032. [PubMed: 10514488]

Shimomura I, Bashmakov Y, Ikemoto S, Horton JD, Brown MS, Goldstein JL. Insulin selectively increases SREBP-1c mRNA in the livers of rats with streptozotocin-induced diabetes. Proc Natl Acad Sci USA. 1999b; 96:13656–13661. [PubMed: 10570128]

Taghibiglou C, Carpentier A, Van Iderstine SC, Chen B, Rudy D, Aiton A, Lewis GF, Adeli K. Mechanisms of hepatic very low density lipoprotein overproduction in insulin resistance. Evidence for enhanced lipoprotein assembly, reduced intracellular ApoB degradation, and increased microsomal triglyceride transfer protein in a fructose-fed hamster model. J Biol Chem. 2000; 275:8416–8425. [PubMed: 10722675]

Yang J, Goldstein JL, Hammer RE, Moon YA, Brown MS, Horton JD. Decreased lipid synthesis in livers of mice with disrupted Site-1 protease gene. Proc Natl Acad Sci USA. 2001; 98:13607–13612. [PubMed: 11717426]

Ye J. Cell biology. Protease sets site-1 on lysosomes. Science. 2011; 333:50–51. [PubMed: 21719668]
Zhang Y, Proenca R, Maffei M, Barone M, Leopold L, Friedman JM. Positional cloning of the mouse obese gene and its human homologue. Nature. 1994; 372:425–432. [PubMed: 7984236]

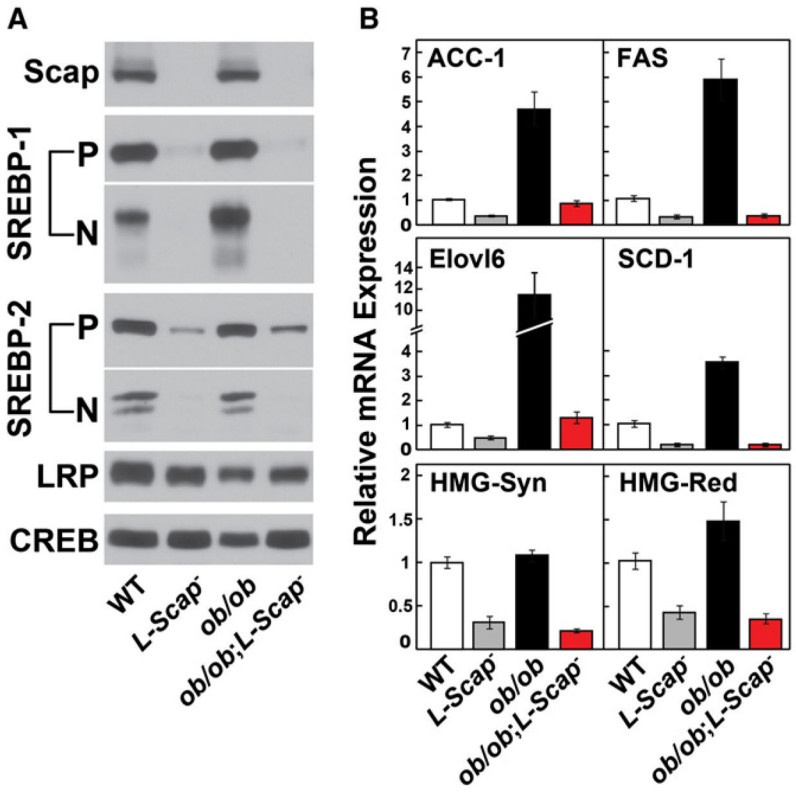

Figure 1. Liver Protein and mRNA Levels in WT, *L-Scap*$^{-}$, *ob/ob,* and *ob/ob;L-Scap*$^{-}$Mice

(A and B) Mice used are described in Table S1. (A) Liver membrane and nuclear extract proteins were prepared from five to six mice per group. Equal aliquots from each mouse were pooled (total, 20 μg for membranes and 30 μg for nuclear extracts) and subjected to 8% SDS-PAGE and immunoblot analysis. LRP and CREB proteins were used as loading controls for membrane and nuclear extract fractions, respectively. P, membrane precursor; N, nuclear form. (B) Total RNA was isolated from each mouse liver and subjected to quantitative real-time PCR using β-actin as the invariant control. Each value represents mean ± SEM of five to six mice relative to WT controls, which was arbitrarily defined as 1.0. Statistical analysis was performed with two-tailed Student's t test. ACC-1, acetyl-CoA carboxylase-1; FAS, fatty acid synthase; Elovl6, elongation of very long chain fatty acids 6; SCD-1, stearoyl-CoA desaturase-1; HMG-CoA Syn, HMG-CoA synthase; HMG-CoA Red, HMGCoA reductase.

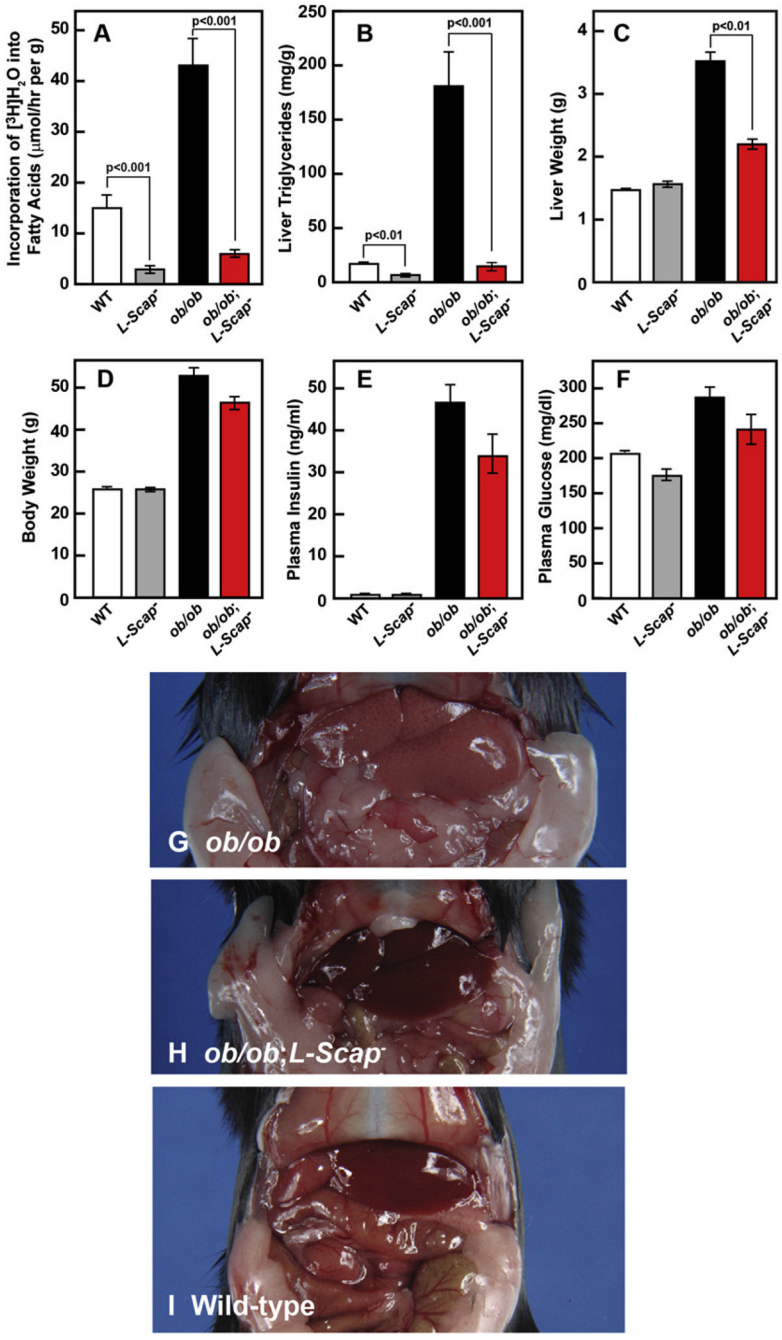

Figure 2. Liver-Specific Deletion of *Scap* Blocks FA Synthesis and Prevents Hepatic Steatosis in *ob*/*ob* Mice

(A) In vivo synthesis rates of FAs in livers of WT, *L-Scap*$^{-}$, *ob*/*ob,* and *ob*/*ob;L-Scap*$^{-}$ mice. Chow-fed male mice (16 weeks old) of the indicated genotype were injected intraperitoneally with ^{3}H-labeled water (50 mCi in 0.25 ml of isotonic saline). One hr later, liver was removed for measurement of ^{3}H-labeled FAs as described (Shimano et al., 1996). Rates of FA synthesis were calculated as μmoles of ^{3}H-radioactivity incorporated into FAs per hr per g liver. Each bar represents mean ± SEM of values from four to six mice.

(B) TG concentrations in livers of 12-week-old male mice with the indicated genotypes. Mice used were those described in Table S1. Each bar represents mean ± SEM of data from five to six mice.
(C) Liver weights of mice in (B).
(D) Body weights of mice in (B).
(E) Plasma insulin concentrations of mice in (B).
(F) Plasma glucose concentrations of mice in (B).
(G–I) Representative photographs of 20-week-old *ob*/*ob*
(G) and *ob*/*ob;L-Scap*$^{-}$ (H), and WT (I) mice.

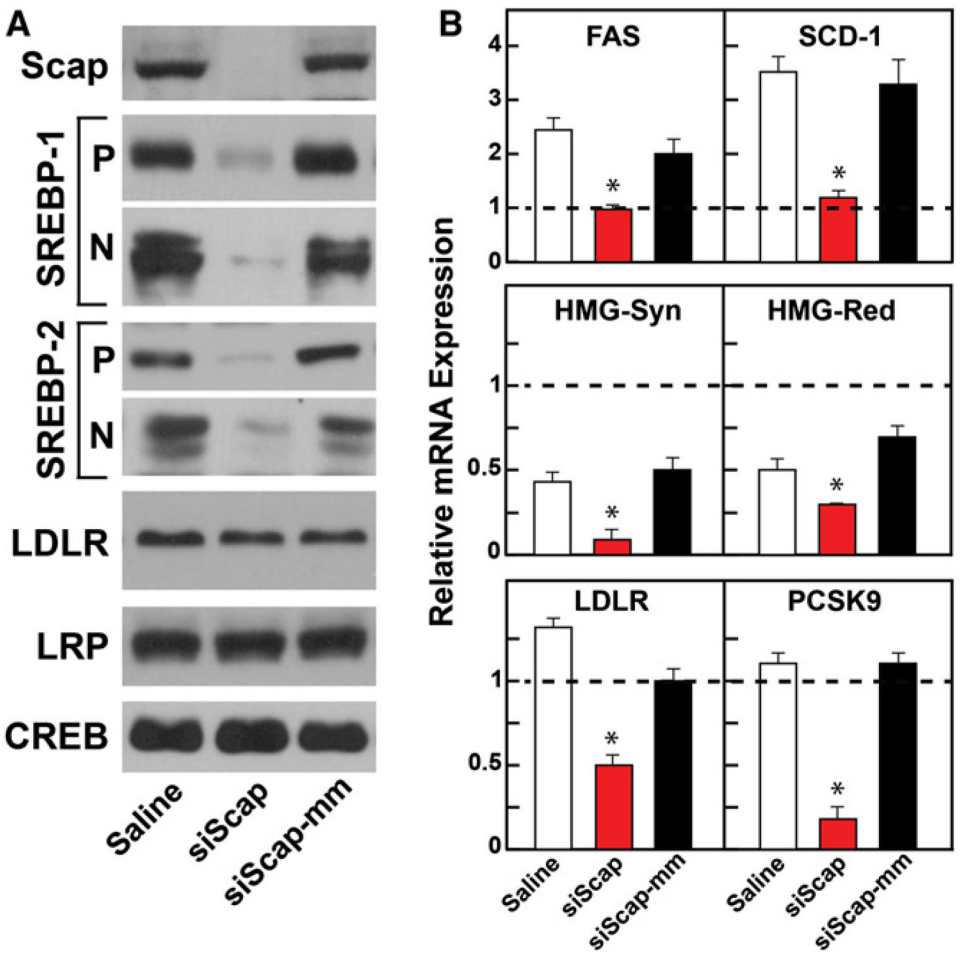

Figure 3. RNAi-Mediated Silencing of Scap in Hamsters

(A and B) Hamsters used are described in Table S2. Hamsters were fed chow or a high-sucrose diet for 7 weeks and injected with saline, siScap, or siScap-mm on weeks 4 and 6. (A) Membrane and nuclear extract fractions prepared individually from six to seven hamster livers per treatment group. Equal aliquots of protein from each liver were pooled (total, 30 μg) and subjected to 8% SDS-PAGE and immunoblot analysis. LRP and CREB proteins were used as loading controls for membrane and nuclear extract fractions, respectively. P, membrane precursor; N, nuclear form. (B) Total RNA was isolated from each hamster liver and subjected to quantitative real-time PCR using β-actin as the invariant control. Each value represents mean ± SEM relative to chow-fed hamsters injected with saline, which was arbitrarily defined as 1.0 and shown as a dashed line. *$p < 0.01$ denotes the level of statistical significance (two-tailed Student's t test) between saline- and siScap-injected hamsters fed the sucrose diet.

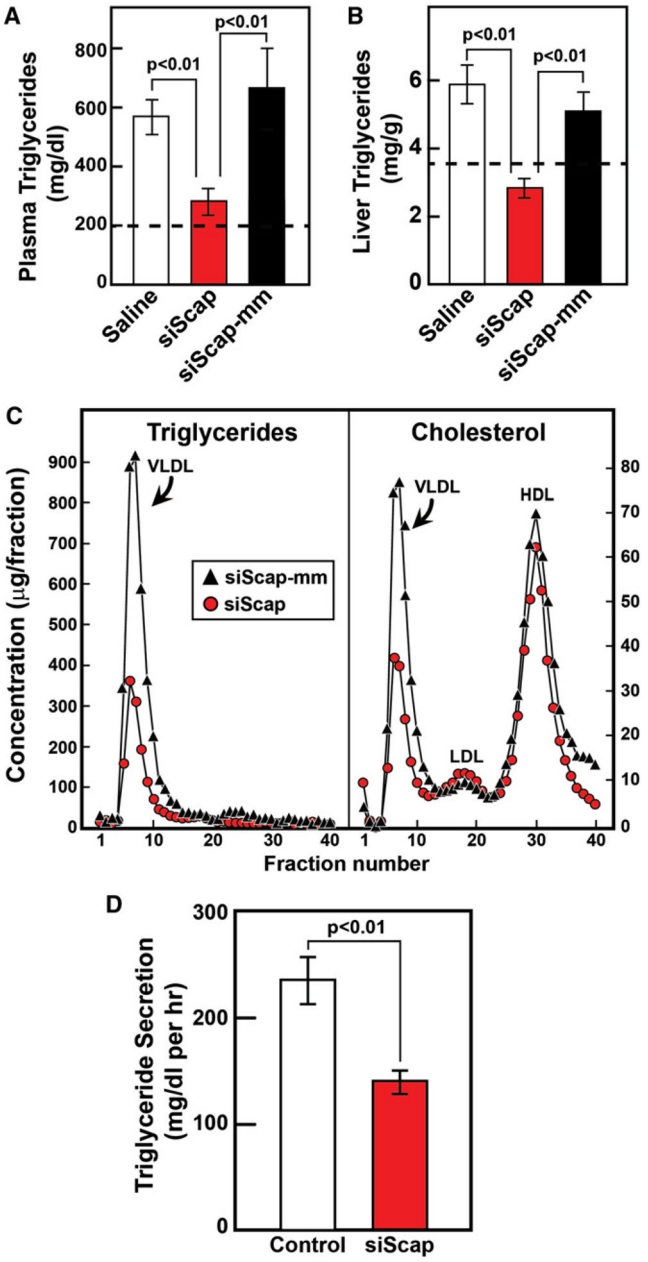

Figure 4. RNAi-Mediated Silencing of Scap Prevents Hepatic Steatosis and Hyperlipidemia in Sucrose-Fed Hamsters

(A–C) Hamsters used in (A)–(C) are described in Table S2. (A) Plasma TG concentrations in hamsters injected with saline, siScap-mm (control), or siScap. Each value represents the mean ± SEM of six to seven hamsters. The dashed line represents the level measured in hamsters fed standard chow. (B) Liver TG concentrations of hamsters described in (A). (C) FPLC profiles of plasma lipoproteins from hamsters injected with siScap-mm or siScap. Equal aliquots of plasma from six to seven hamsters in each group was pooled and subjected to gel filtration by FPLC. Concentrations of TGs and cholesterol in each fraction were measured as described in Experimental Procedures.

(D) RNAi-mediated silencing of Scap reduces TG secretion from liver. Hamsters were fed a high-sucrose diet for 7 weeks. On weeks 4 and 6, hamsters were injected with 2.5 mg/kg

body weight of LNP-formulated siLuciferase (Control) or siScap. One week after the final injection, hamsters were anesthetized with pentobarbital (40 mg/kg) and injected with 20% Tyloxapol (600 mg/kg body weight). Blood samples were obtained at times 0 and 100 min following injection of Tyloxapol. The difference in plasma TG concentrations between the two time points was used to calculate the rate of TG secretion, which was expressed as mg/dl per hr. Each bar represents the mean ± SEM of data from six hamsters. Statistical analysis was performed with the two-tailed Student's t test.